SUPPLEMENTARY TEXT

Supplementary Materials and Methods

Mice and human pituitaries

Mice and embryos were genotyped using an ear or tail biopsy, respectively. DNA was extracted using a 20ul solution of a 1 in 5 dilution of DNAreleasy (Anachem) according to the manufacturer's instructions. The data presented in this work is representative from at least 3 individual embryos per genotype. All animal procedures were carried out under the Animals (Scientific Procedures) fully compliant with the current Home Office legislation.

Histology and *in situ* hybridisation on histological sections

The antisense riboprobes used in this study (*Shh*, *Bmp4*, *Fgf8*, *Lhx3*, *Lhx4*, *Pax6*, *Six3*, *Wnt5a*, *Tbx2*, *Tbx3*, *Nxk2.1*, *Pomc1*, *Ghrh*, *Gnrh*, *Ss*, *Ot* and *Gnrh*) have been described previously (Gaston-Massuet et al., 2011; Jayakody et al., 2012; Trowe et al., 2013). Full-length human antisense riboprobe against *GLI1* was obtained from Source Bioscience (BE296931).

Immunofluorescence

Detection of hormones were carried out using antibodies for GH (NHPP AFP-5641801), ACTH (10C-CR1096M1), TSH (NHPP AFP-1274789), PRL (NHPP AFP-425-10-91), LH (NHPP AFP-C697071P) and FSH (AFP-7798-1289) (Developmental Studies Hybridoma Bank) at a 1:1000 dilution. Detection of pituitary lineage commitment markers was performed using antibodies for PIT1 (Gift from S. Rhodes), TPIT (Gift from J. Drouin) and GSU (Developmental Studies Hybridoma Bank) at a 1:1000 dilution. of 1:200. Markers of pituitary stem cells-SOX2 (GT15098, Immune Systems) and SOX9 (AB5535, Milipore) were used at a dilution of 1:250 and 1:500, respectively. Cruz). Detection of activated BMP4 and FGF responding cells was performed using pERK1/2 (9101, Cell Signaling) and pSMAD1/5/8 (41D10, Cell Signaling) at a dilution of 1:250. Proliferation marker pHH3 was

used at a 1:155 dilution (06-570, Millipore). Pituitary markers PITX1 (Gift from J. Drouin), LHX3 (67.4E12, Developmental Studies Hybridoma Bank) and ISL1 (K-20, Santa Cruz) were used at a dilution of 1:1000. Anterior hypothalamic markers SHH (AF464, R&D Systems), TCF4 (05-511, Millipore) and OTX2 (sc-514195, Santa Cruz) were used at a dilution of 1:100. N-cadherin (ab18203, Abcam) and E-cadherin (610181, BD BioScience) were used at a 1:100 dilution. Histological sections were counterstained with DAPI (Sigma).

RNA sequencing of dissected Rathke's pouch epithelium

Rathke's pouch was dissected from wild-type embryos at 10.5 dpc. RNA was extracted using RNeasy Micro Kit (Qiagen). RNA quality and concentration was measured using the 2100 Bioanalyzer. Extracted RNA was then sent to Wellcome Trust Genomics unit, Oxford University for RNA sequencing. Library preps made using the Smarter kit (High Vol #634828) from Clonetech/Takara and PolyA-Illumina's TruSq stranded kit (RS-122-2103 #E6040L) from New England Bioloabs. RNA sequencing was performed using the SMARTer-seq low input RNA kit. RNA sequencing parameters were 80bp, double ends and 15 million read depth with amplification. Alignment against mm10 reference genome was performed using Stampede. Per gene read counts were calculated using RSubread, differential analyses was performed using DESEq2 and ontology analysis using GOSeq (Liao et al., 2013; Love et al., 2014; Young et al., 2010). For gene set enrichment analysis (GSEA), genes were ranked by their Wald statistic and GSEA performed using the pre-ranked tool in GSEA v2.2.3 (Broad Institute) (Subramanian et al., 2005). The Hallmark Sonic Hedgehog pathway geneset was downloaded from the Molecular Signature Database v5.2 (Broad Institute) (Subramanian et al., 2005).

Assessment of clonogenic potential

Pituitaries were dissected using aseptic forceps and the posterior pituitary was removed. The anterior lobe was minced with forceps and placed into 200ul of Enzyme mix, which consists of Hanks' Balanced Salt Solution (HBSS, Gibco), 0.5% w/v Collagenase (Worthington),

50ug/ml (Worthington), 1% Fungizone and 0.1X trypsin (Sigma), for 4 hours in a 37ºC water bath. HBSS was added to make a final volume of 500ul post incubation and the solution was triturated into a single cell suspension. Once single cell suspension was achieved, 9.5ml of HBSS is added and the cells are spun down for 5 minutes at 1000rpm. Cells were re-suspended in growth medium, which consists of DMEM/F12, 5% FCS, 1% PenStrep, 20ng/ml human recombinant bFGF (R&D Systems) and 50ng/ml cholera toxin. Cells were plated at clonal density in a 6-well plate at 2000, 4000 and 8000 cells per well. Media was changed every 3 days after colony establishment. To count the number of colonies, after 7 days, colonies were washed with 1X PBS and fixed for 20 minutes with 4% PFA. Colonies were stained with Harris' haematoxylin for 15 minutes at RT. The proportion of colonies observed relative to seeded cells was used to estimate total clonogenic cells in 18.5 dpc pituitaries by multiplying this value with the total number of cells in the dissociated pituitary.

Table S1. Pituitary Gene Ontology

Category	over_repr	numDEIn	numInCat	term	ontology	padj
GO:00219	0.000167	4	38	Pituitary	BP	0.046803

Table S2. Genes involved in pituitary development.

*Fold Change	Gene Symbol	Adjusted p-value
4.231324889	*Pitx1*	0.006657901
5.105959333	*Prop1*	0.000884996
1.575755361	*Bmp2*	0.999855699
27.69985383	*Lhx4*	5.74E-21
16.90654044	*Lhx3*	3.31E-14
44.21160974	*Hesx1*	2.99E-30
0.639540028	*Pax6*	0.999855699
1.031192461	*Sox2*	0.999855699
0.091398855	*Pax3*	2.73E-09
0.892479935	*Tcf3*	0.999855699
1.96329081	*Six3*	0.488932014
1.459287982	*Isl1*	0.999855699

* higher than 1.0 means up-regulated in the wild-type RP

Supplementary References

Gaston-Massuet, C., Andoniadou, C. L. C. L., Signore, M., Jayakody, S. a, Charolidi, N., Kyeyune, R., Vernay, B., Jacques, T. S., Taketo, M. M., Le Tissier, P., et al. (2011). Increased Wingless (Wnt) signaling in pituitary progenitor/stem cells gives rise to pituitary tumors in mice and humans. *Proc. Natl. Acad. Sci. U. S. A.* **108**, 11482–11487.

Jayakody, S. A., Andoniadou, C. L., Gaston-massuet, C., Signore, M., Cariboni, A., Bouloux, P. M., Tissier, P. Le, Pevny, L. H., Dattani, M. T. and Martinez-barbera, J. P. (2012). SOX2 regulates the hypothalamic-pituitary axis at multiple levels. *J. Clin. Invest.* **122**, 3635–3646.

Liao, Y., Smyth, G. K. and Shi, W. (2013). The Subread aligner: fast, accurate and scalable read mapping by seed-and-vote. *Nucleic Acids Res.* **41**, e108.

Love, M. I., Huber, W. and Anders, S. (2014). Moderated estimation of fold change and dispersion for RNA-seq data with DESeq2. *Genome Biol.* **15**, 550.

Subramanian, A., Tamayo, P., Mootha, V. K., Mukherjee, S., Ebert, B. L., Gillette, M. A., Paulovich, A., Pomeroy, S. L., Golub, T. R., Lander, E. S., et al. (2005). Gene set enrichment analysis: A knowledge-based approach for interpreting genome-wide expression profiles. *Proc. Natl. Acad. Sci.* **102**, 15545–15550.

Trowe, M.-O., Zhao, L., Weiss, A.-C., Christoffels, V., Epstein, D. J. and Kispert, A. (2013). Inhibition of Sox2-dependent activation of Shh in the ventral diencephalon by Tbx3 is required for formation of the neurohypophysis. *Development* **140**, 2299–2309.

Young, M. D., Wakefield, M. J., Smyth, G. K., Oshlack, A., Fu, X., Fu, N., Guo, S., Yan, Z., Xu, Y., Hu, H., et al. (2010). Gene ontology analysis for RNA-seq: accounting for selection bias. *Genome Biol.* **11**, R14.

Supplementary Figures

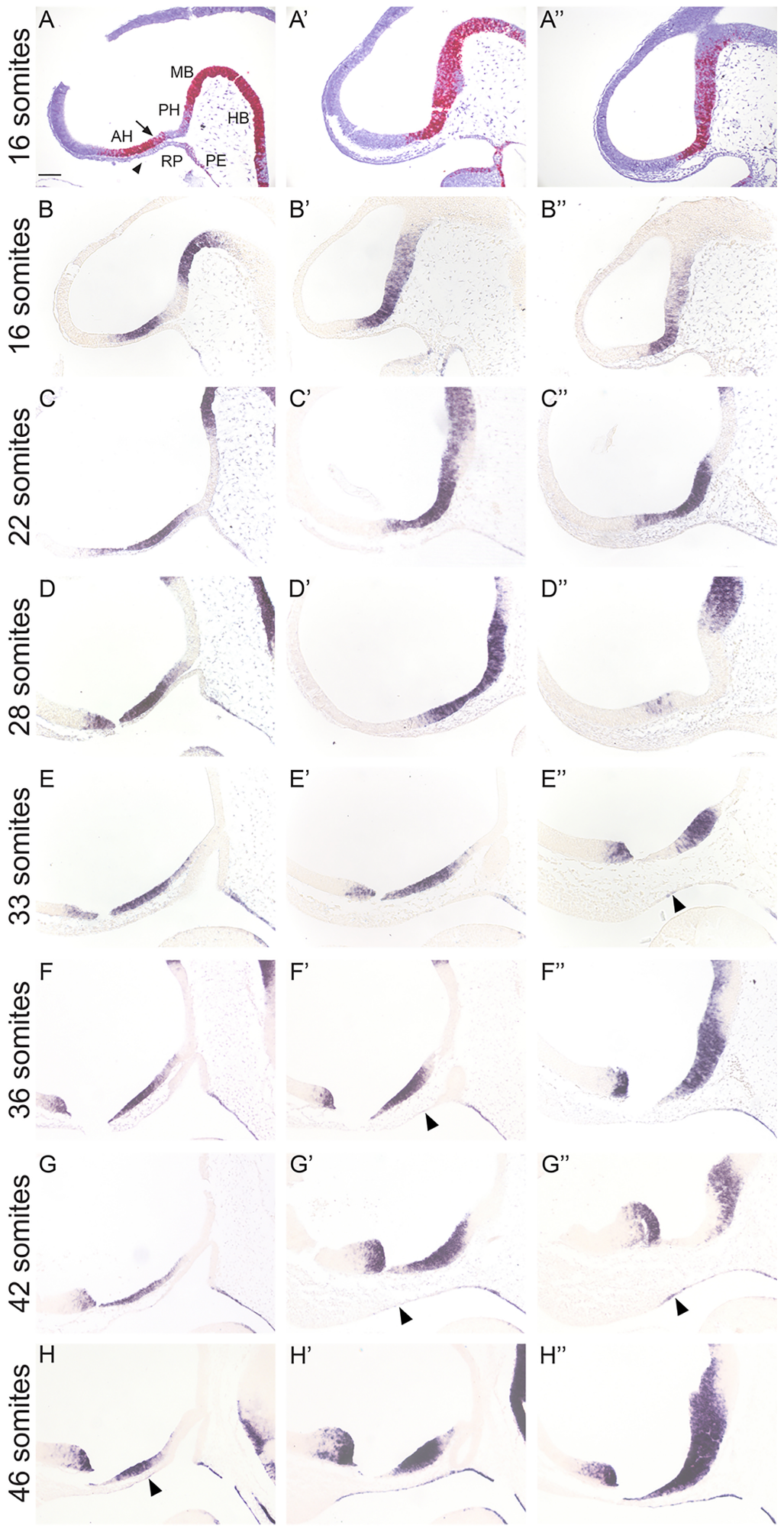

Figure S1. *Shh* is expressed in the oral ectoderm in wild-type embryos by the 33 somite stage. RNA *in situ* hybridisation on sagittal histological sections of wild-type embryos between 16 and 46 somites. Three different levels are shown from approximately midline sagittal (A-H), medio-lateral (A′-H′) and lateral (A′′-H′′). (**A-D**) From 16 to 28 somites *Shh* transcripts are detected in the midline anterior hypothalamus (AH, arrow), posterior hypothalamus (PH) and pharyngeal endoderm (PE) abutting the developing Rathke's pouch (RP). No expression is observed in the developing oral ectoderm at these stages (arrowhead). (**E**) At 33 somites, *Shh* transcripts are weakly detected in the lateral oral ectoderm (arrowhead) and pharyngeal endoderm. (**F-H**) Stronger *Shh* expression is observed in the medio-lateral and lateral oral ectoderm from the 36 somite-stage (arrowheads). Abbreviations: RP, Rathke's pouch; PH, posterior hypothalamus; AH, anterior hypothalamus; PE, pharyngeal endoderm; MB, midbrain; HB, hindbrain. Scale bar is 100μm.

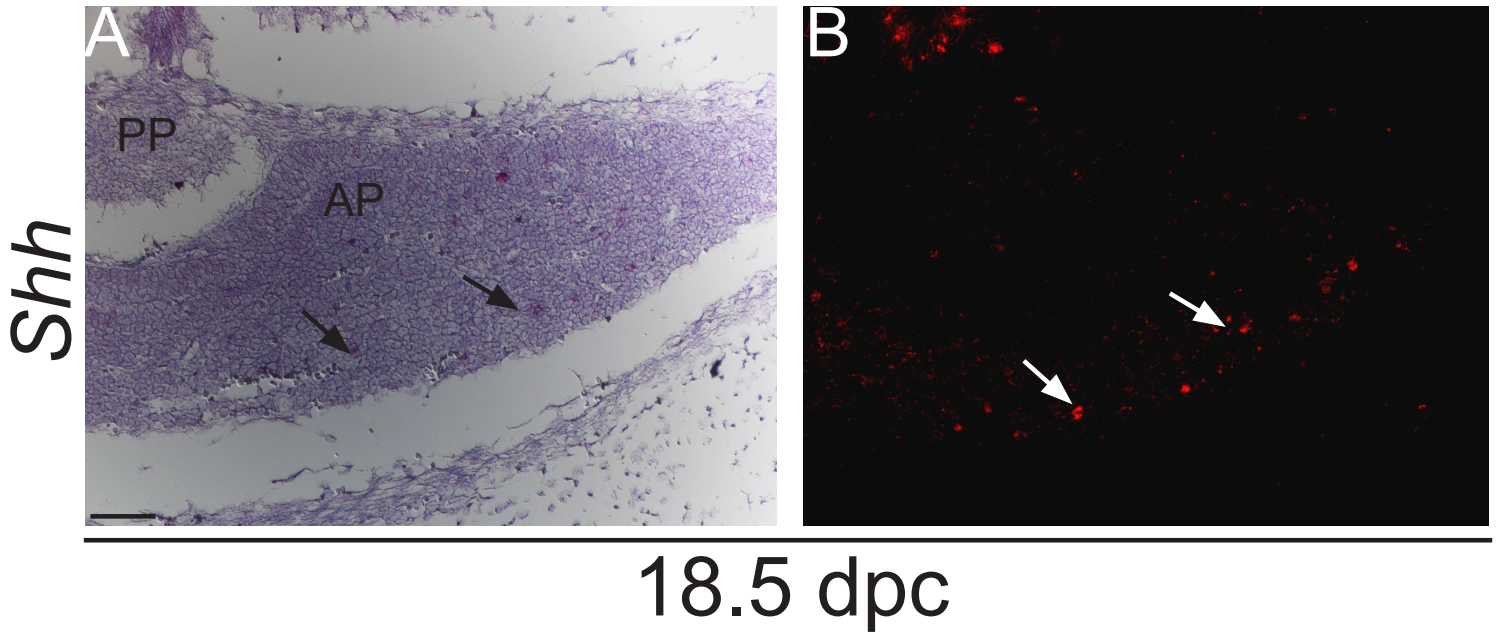

Figure S2. *Shh* mRNA is detectable in single cells within the anterior pituitary at 18.5 dpc. (A,B) RNA *in situ* hybridisation using the RNAscope (ACDBio) procedure on frontal sections of wild-type embryos at the level of the pituitary gland. Note the presence of positive foci within the anterior pituitary in both the bright field (A) and fluorescent picture (B) (arrows).

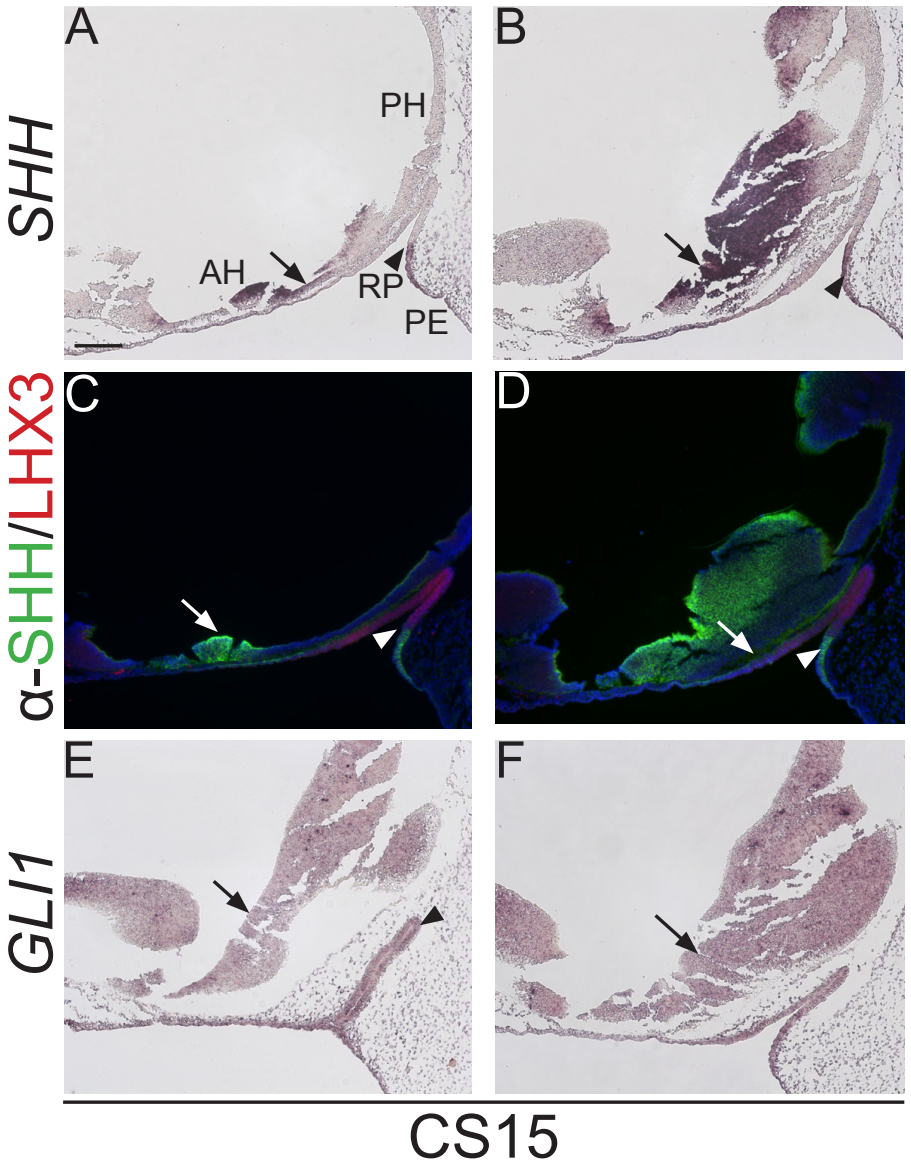

Figure S3. *SHH* and *GLI1* are expressed in human fetal pituitaries. *In situ* hybridisation and double immunofluorescence on two non-consecutive mid sagittal sections of human fetal pituitaries at Carnegie stage 15 (CS15). (**A,B**) *SHH* transcripts are expressed in the anterior hypothalamus (AH, arrows) and pharyngeal endoderm (PE), but not in the developing Rathke's pouch (RP) (arrowheads). (**C,D**) SHH immunostaining (green signal) confirms the expression in the AH (arrow) and PE, but not in RP, which is positive for LHX3 (red signal). (**E,F**) *GLI1* transcripts are found throughout the hypothalamus (arrows) and RP (arrowheads). Abbreviations: AH, anterior hypothalamus; RP, Rathke's pouch; PE, pharyngeal endoderm; PH, posterior hypothalamus. Scale bar: 100µm.

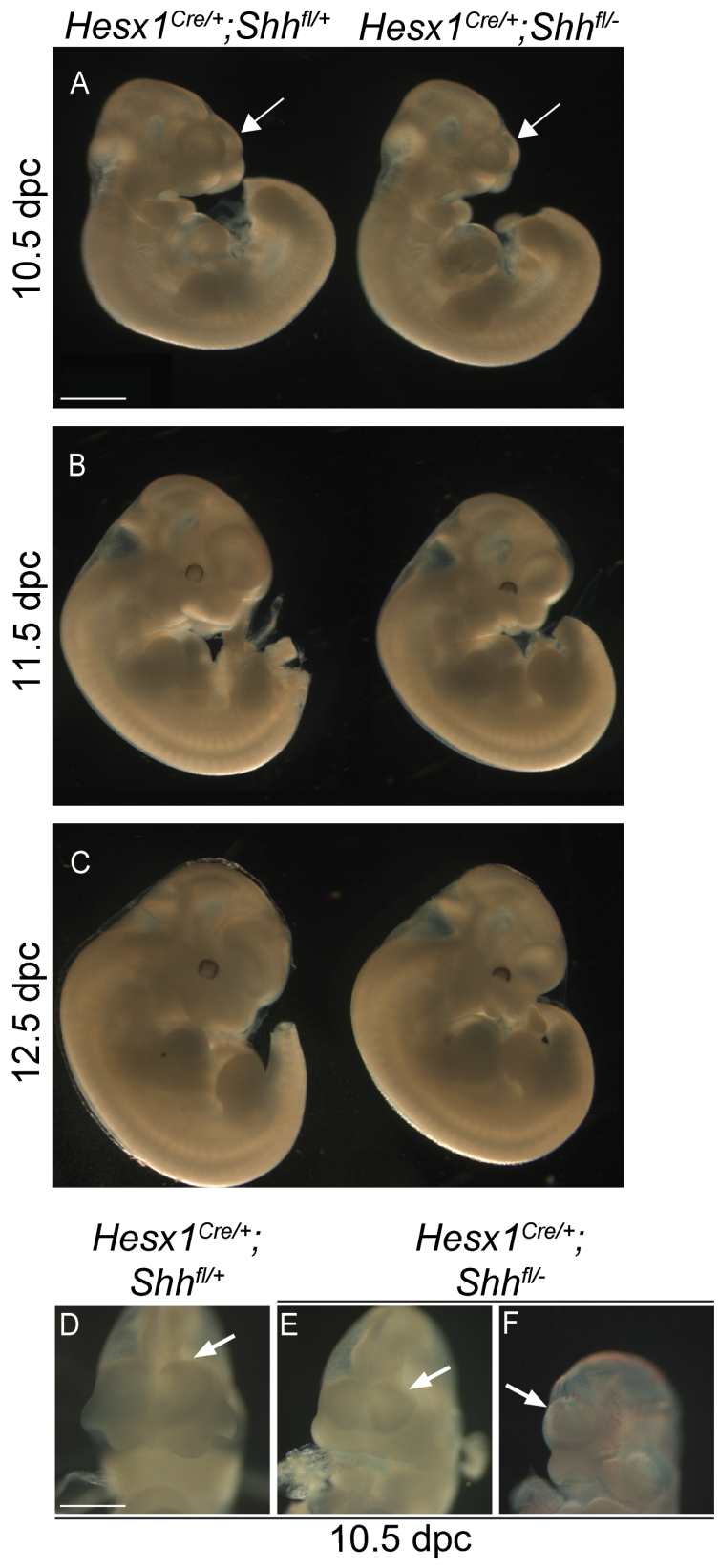

Figure S4. Forebrain defects in *Hesx1$^{Cre/+}$;Shh$^{fl/-}$* embryos. (**A-F**) *Hesx1$^{Cre/+}$;Shh$^{fl/+}$ and Hesx1$^{Cre/+}$;Shh$^{fl/-}$* embryos from 10.5 to 12.5 dpc showing small telencephalic vesicles (arrows) and eye defects. (**G-I**) Frontal view a control embryo and two *Hesx1$^{Cre/+}$;Shh$^{fl/-}$* mutants at 10.5 dpc, showing the small telencephalic vesicles (H) and holoprosencephaly (I). Scale bar: 1mm.

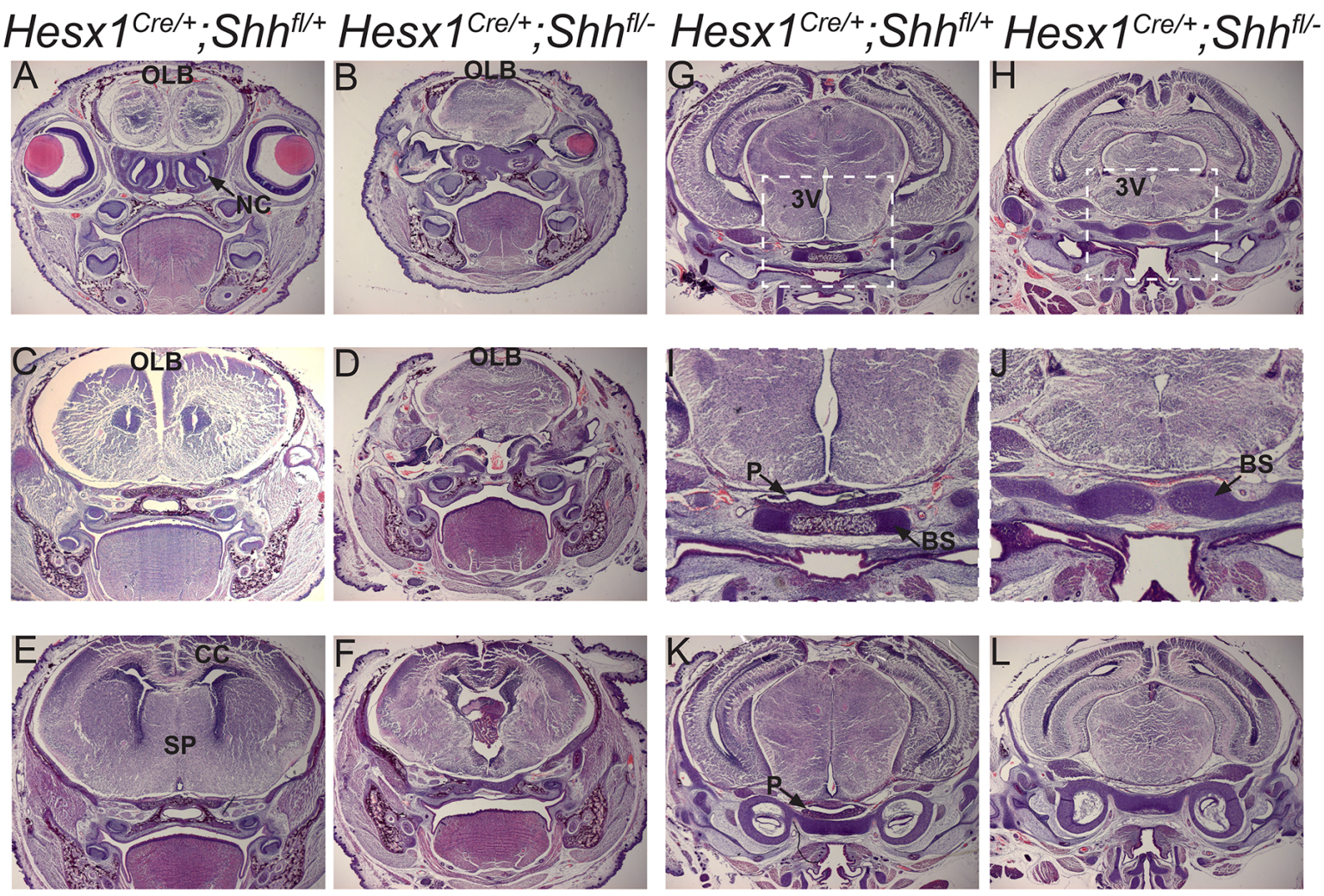

Figure S5. Craniofacial defects and loss of pituitary tissue in *Hesx1*$^{Cre/+}$;*Shh*$^{fl/-}$ mutants at 18.5 dpc. Haematoxylin and eosin (H&E) staining on frontal sections from the eyes to the posterior hypothalamus in *Hesx1*$^{Cre/+}$;*Shh*$^{fl/-}$ mutant and control embryos at 18.5 dpc. (**A-F**) *Hesx1*$^{Cre/+}$;*Shh*$^{fl/-}$ mutants show eye defects (microphthalmia or anophthalmia), fused olfactory bulbs (OLB), deformed nasal cavity (NC) and absent of the septum pellucidum (SP) and corpus callossum (CC). (**G-J**) At more posterior levels, the two cerebral hemispheres are identifiable, but the entire brain is smaller in the mutant relative to the control embryo, and the pituitary (P, arrows in I and K) is absent in the mutant. Abbreviations: 3V, third ventricle; BS, basisphenoid bone; NC, nasal cavity; OLB olfactory bulbs; P, pituitary. Scale bar: 100 μm.

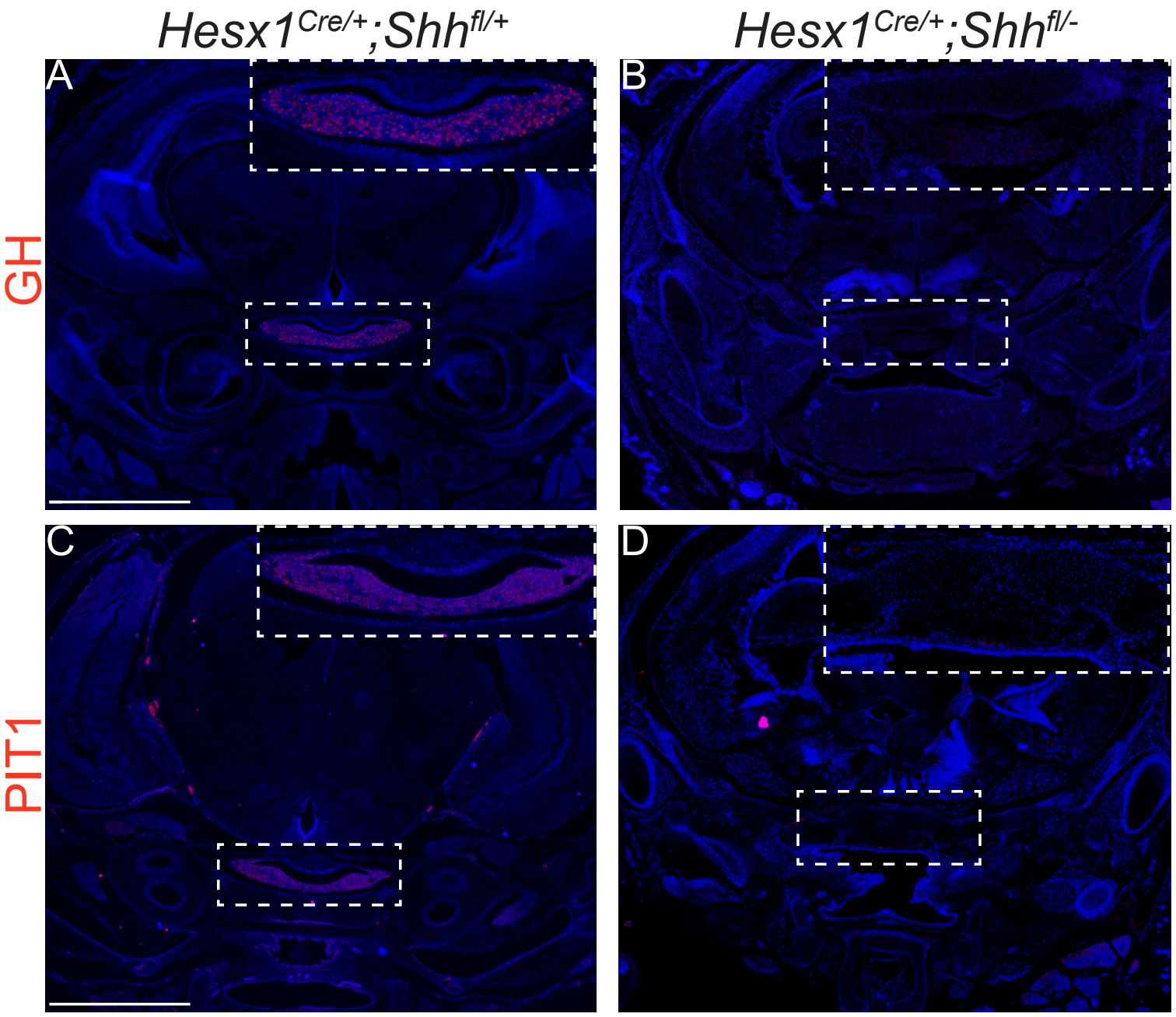

Figure S6. Loss GH+ve and PIT1+ve cells in the *Hesx1*$^{Cre/+}$;*Shh*$^{fl/-}$ mutant pituitary at 18.5 dpc. Immunofluorescence against GH (A,B) and PIT1 (C,D) on frontal sections from control and *Hesx1*$^{Cre/+}$;*Shh*$^{fl/-}$ mutant embryos at 18.5 dpc. No positive signal is detectable in the mutant pituitary. Scale bar: 100 μm.

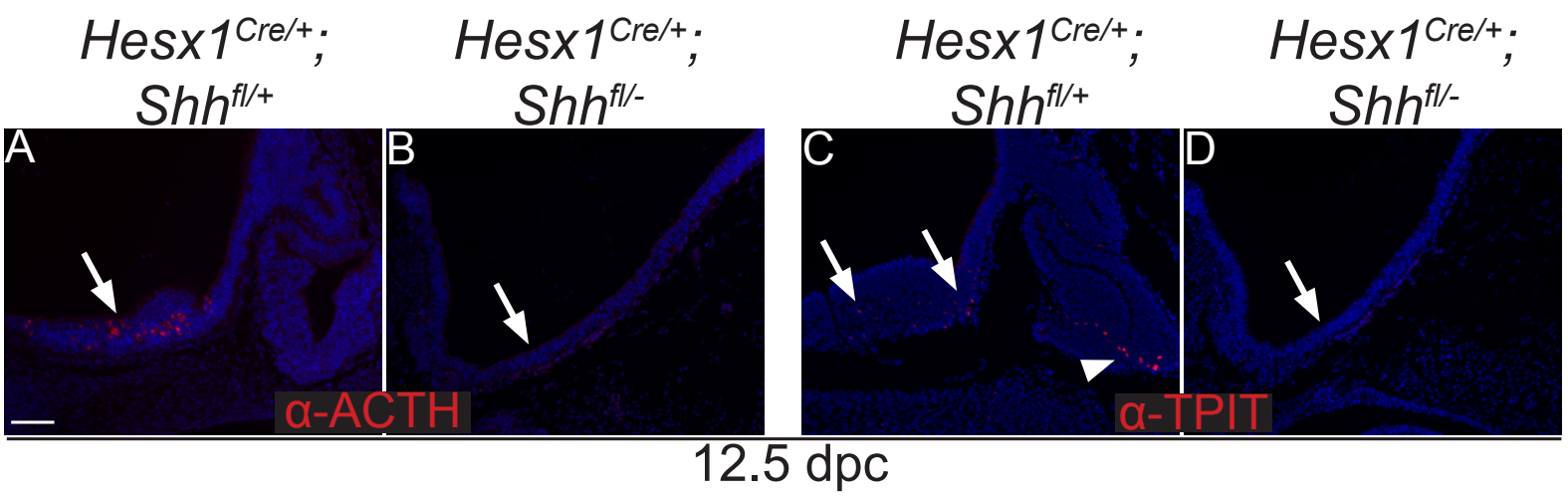

Figure S7. ACTH+ve and TPIT+ve cells are lost in the anterior hypothalamus of *Hesx1$^{Cre/+}$;Shh$^{fl/-}$* mutants. (**A-D**) Immunofluorescence against ACTH (A,B) and TPIT (C,D) on mid-sagittal sections from control and *Hesx1$^{Cre/+}$;Shh$^{fl/-}$* mutant embryos at 12.5 dpc. ACTH+ve and TPIT+ve cells are present in the anterior hypothalamus of control embryos but not *Hesx1$^{Cre/+}$;Shh$^{fl/-}$* mutants (arrows). Note the present of TPIT+ve cells in the control pituitary. Scale bar: 100µm.

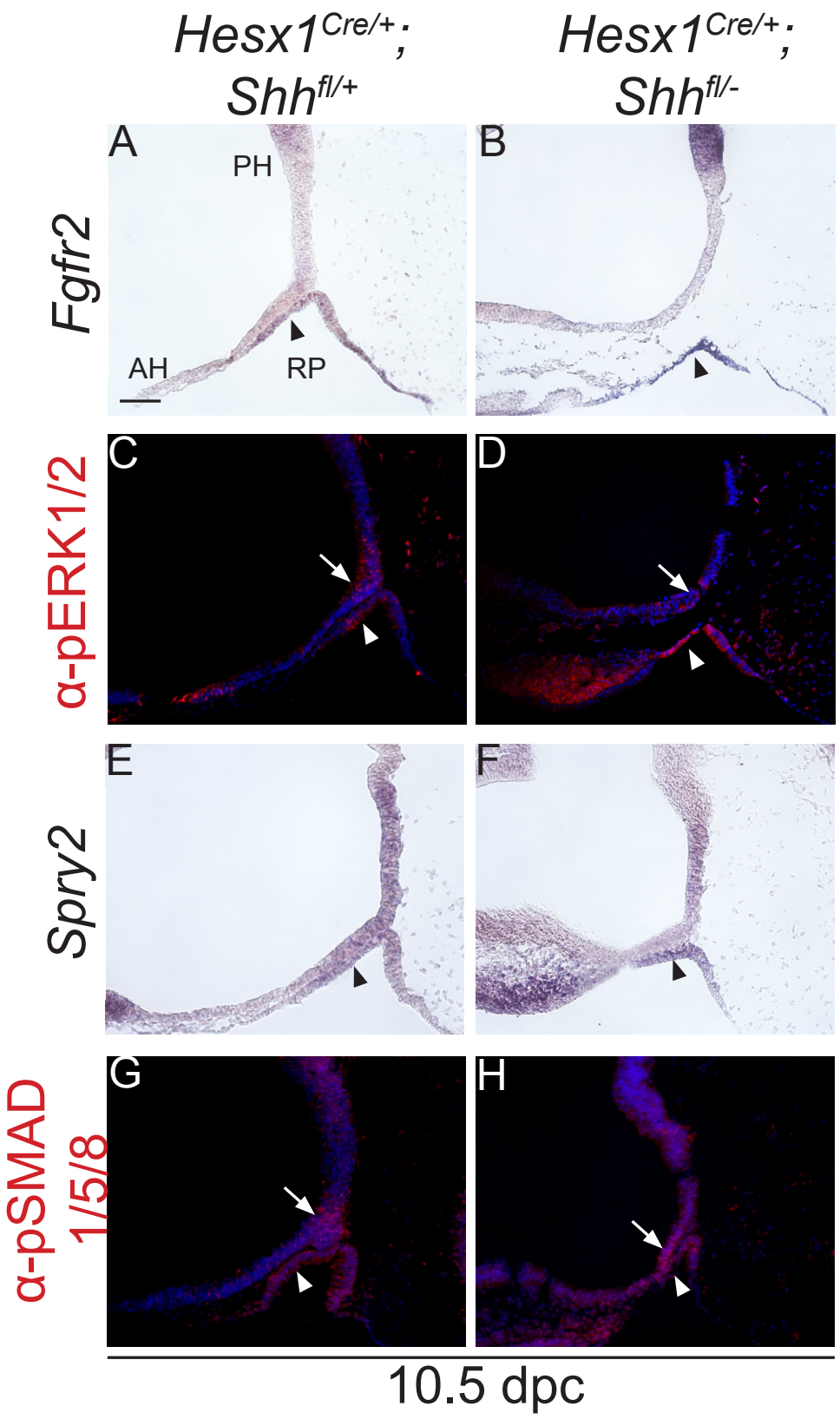

Figure S8. RP is competent to respond to BMP and FGF signalling in *Hesx1*$^{Cre/+}$;*Shh*$^{fl/-}$ mutants. *In situ* hybridisation and immunofluorescence on mid-sagittal sections of *Hesx1*$^{Cre/+}$;*Shh*$^{fl/-}$ mutants and control embryos at 10.5 dpc. (**A,B**) *Fgfr2* transcripts are observed in the control Rathke's pouch (RP) as well as in the rudimentary mutant RP (arrowheads). (**C,D**) Immunofluorescence against p-ERK1/2 reveals positive staining in the hypothalamus and developing RP in both genotypes, suggesting active FGF signalling. (**E,F**) *Spry2*, a direct target of the FGF pathway, is expressed in the hypothalamus and RP in the mutant and control embryo. (**G,H**) Immunofluorescence against p-SMAD1/5/8, a readout of active BMP signalling, showing specific signal in the hypothalamus and RP in both genotypes. Note that head mesenchyme is more abundant in the mutant embryos and expresses pERK1/2, *Spry2* and p-SMAD1/5/8. Scale bar: 100µm.

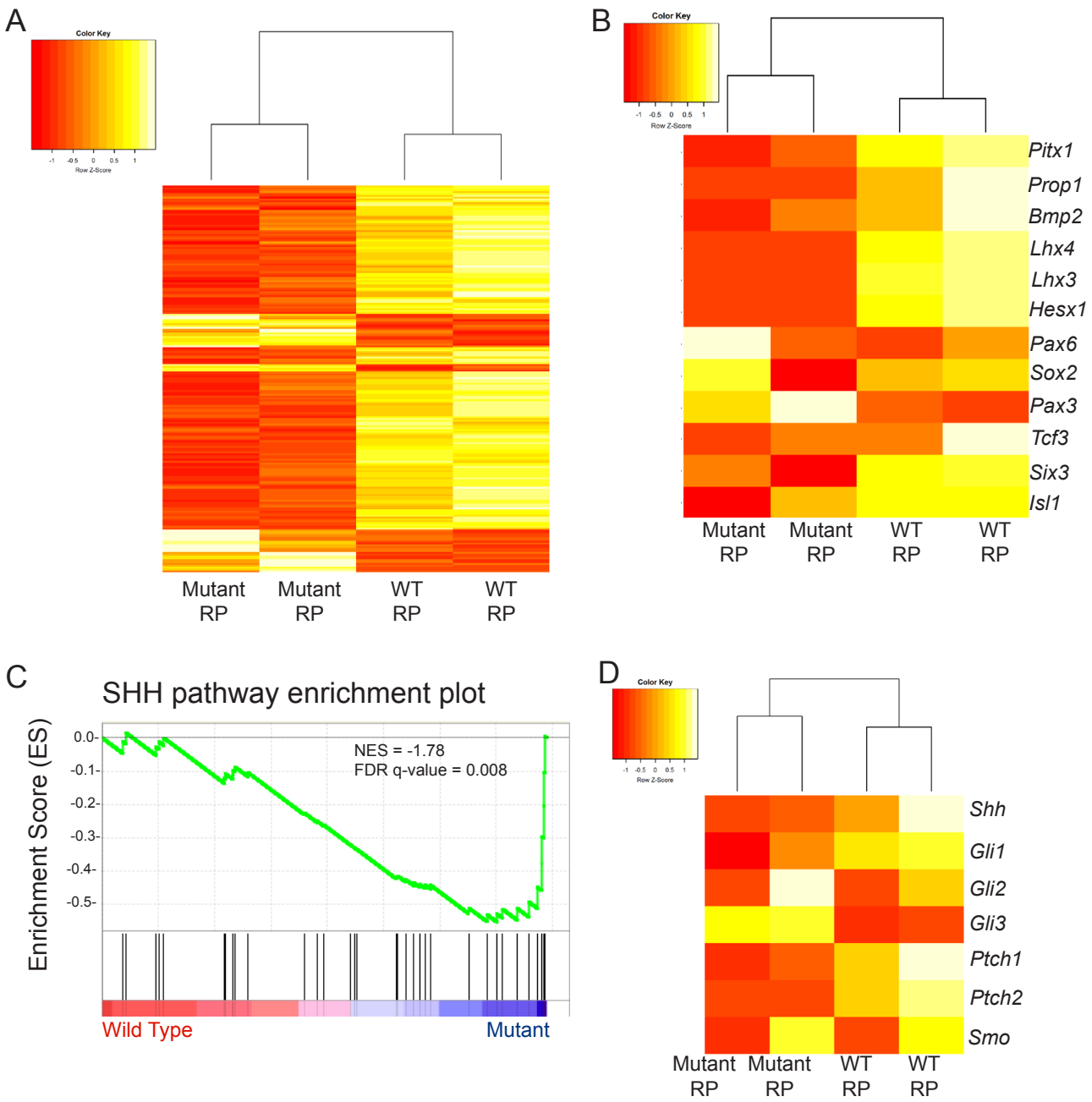

Figure S9. RNA Sequencing data confirms the disruption of RP development in *Hesx1*$^{Cre/+}$;*Shh*$^{fl/-}$ RP at 10.5 dpc. RP from control and mutant embryos (n=2 per group) were manually dissected at 10.5 dpc and subjected to RNA-Sequencing. (**A**) Heatmap representation of the 208 significantly differentially expressed genes between in *Hesx1*$^{Cre/+}$;*Shh*$^{fl/-}$ mutant and control RPs. (**B**) Heatmap representation of 12 functionally important genes during RP and pituitary development, including *Lhx3* and *Lhx4*, revealing the overall down-regulation in their expression levels in the *Hesx1*$^{Cre/+}$;*Shh*$^{fl/-}$ mutant compared with the control RPs. (**C**) Gene set enrichment analysis (GSEA) of differentially expressed genes in mutant RP revealing a negative enrichment for the SHH pathway (Broad Institute) NES: Normalised enrichment score. FDR: False discovery rate. (**D**) Heatmap representation of differentially expressed genes involved in the SHH pathway in *Hesx1*$^{Cre/+}$;*Shh*$^{fl/-}$ mutant and control RP. Note the up-regulation of *Gli1*, *Gli2*, *Ptch1*, *Ptch2* and *Smo* expression levels in the control relative to but the mutant RP. Likewise, *Shh* itself is up-regulated in the control data set. In contrast, *Gli3* expression, a negative regulator of the SHH pathway is up-regulated in the *Hesx1*$^{Cre/+}$;*Shh*$^{fl/-}$ mutant RP.

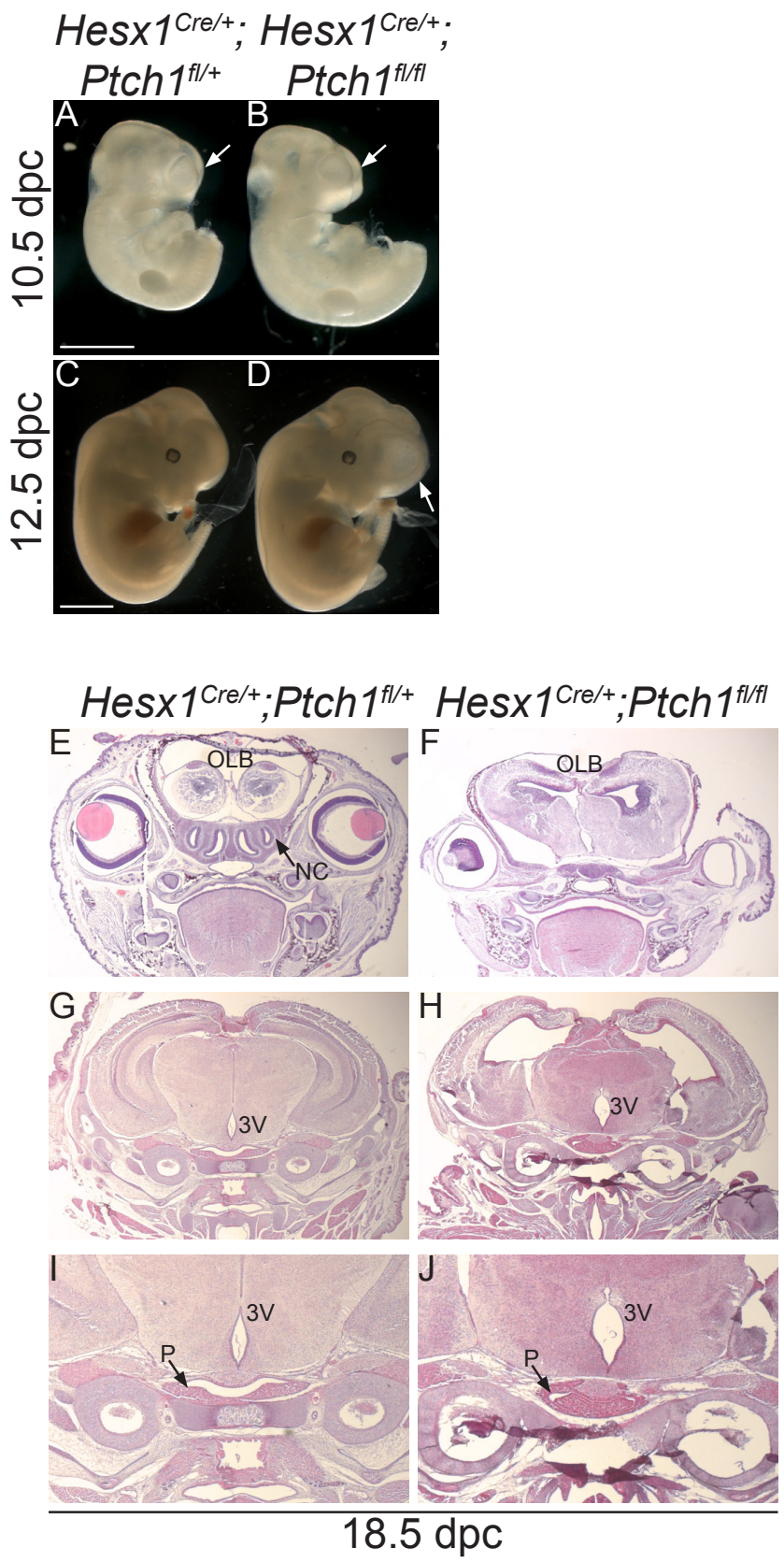

Figure S10. Forebrain and craniofacial defects in the *Hesx1*$^{Cre/+}$;*Ptch1*$^{fl/fl}$ mutants. (**A-D**) *Hesx1*$^{Cre/+}$;*Ptch1*$^{fl/+}$ controls and *Hesx1*$^{Cre/+}$;*Ptch1*$^{fl/fl}$ mutants at 10.5dpc and 12.5 dpc showing the enlargement of the telencephalic vesicles (arrows) . (**E-H**) Haematoxylin and eosin (H&E) staining on frontal sections from the eyes to the posterior hypothalamus in *Hesx1*$^{Cre/+}$;*Ptch1*$^{fl/+}$ controls and *Hesx1*$^{Cre/+}$;*Ptch1*$^{fl/fl}$ mutants at 18.5 dpc. Note the expansion of the olfactory bulbs (OLB), nasal cavity defects (NC) and enlarged pituitary gland (P) in the mutant relative to the control embryo. Scale bar: 100 μm.

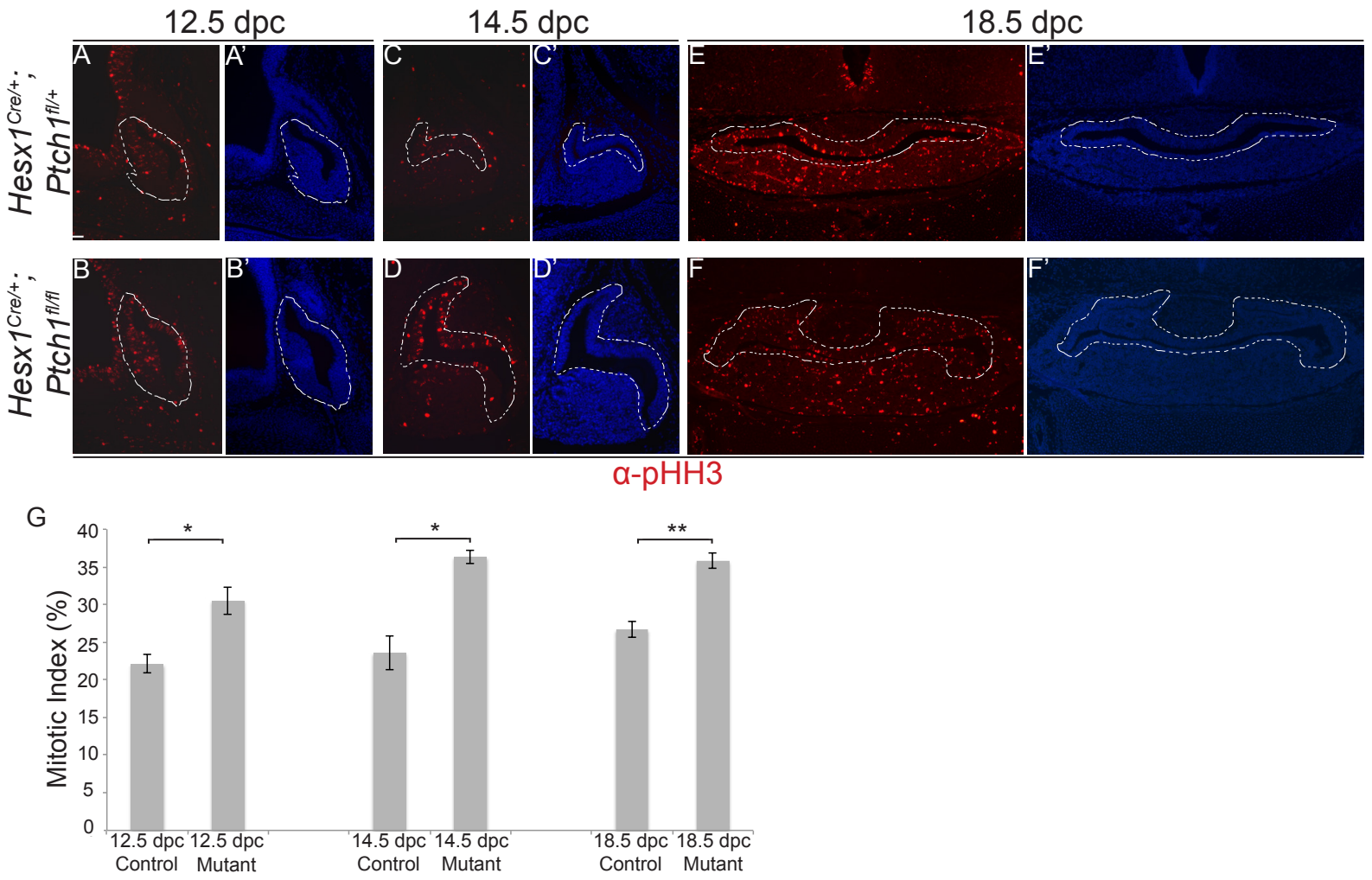

Figure S11. Increased proliferation in *Hesx1*$^{Cre/+}$;*Ptch1*$^{fl/fl}$ pituitaries. (**A-F**) Immunofluorescence against phospho-Histone H3 (pHH3) on mid-sagittal (A-D) and coronal (E,F) sections of control embryos and *Hesx1*$^{Cre/+}$;*Ptch1*$^{fl/fl}$ mutants at 12.5 dpc, when the earliest morphological hyperplasia is visible up, to 18.5 dpc. (**G**) Quantitative analysis revealing the significant increase in the mitotic index in the developing pituitary (i.e. ratio of pHH3+ve cells and DAPI+ve stained nuclei) in the mutants compared with control at all stages analysed. Dashed lines delineate the area that was quantified. Students T-Test: 12.5 dpc, p=0.03; 14.5 dpc, p=0.04; 18.5 dpc, P=0.008; n=6 for each group. Scale bars: 100μm.

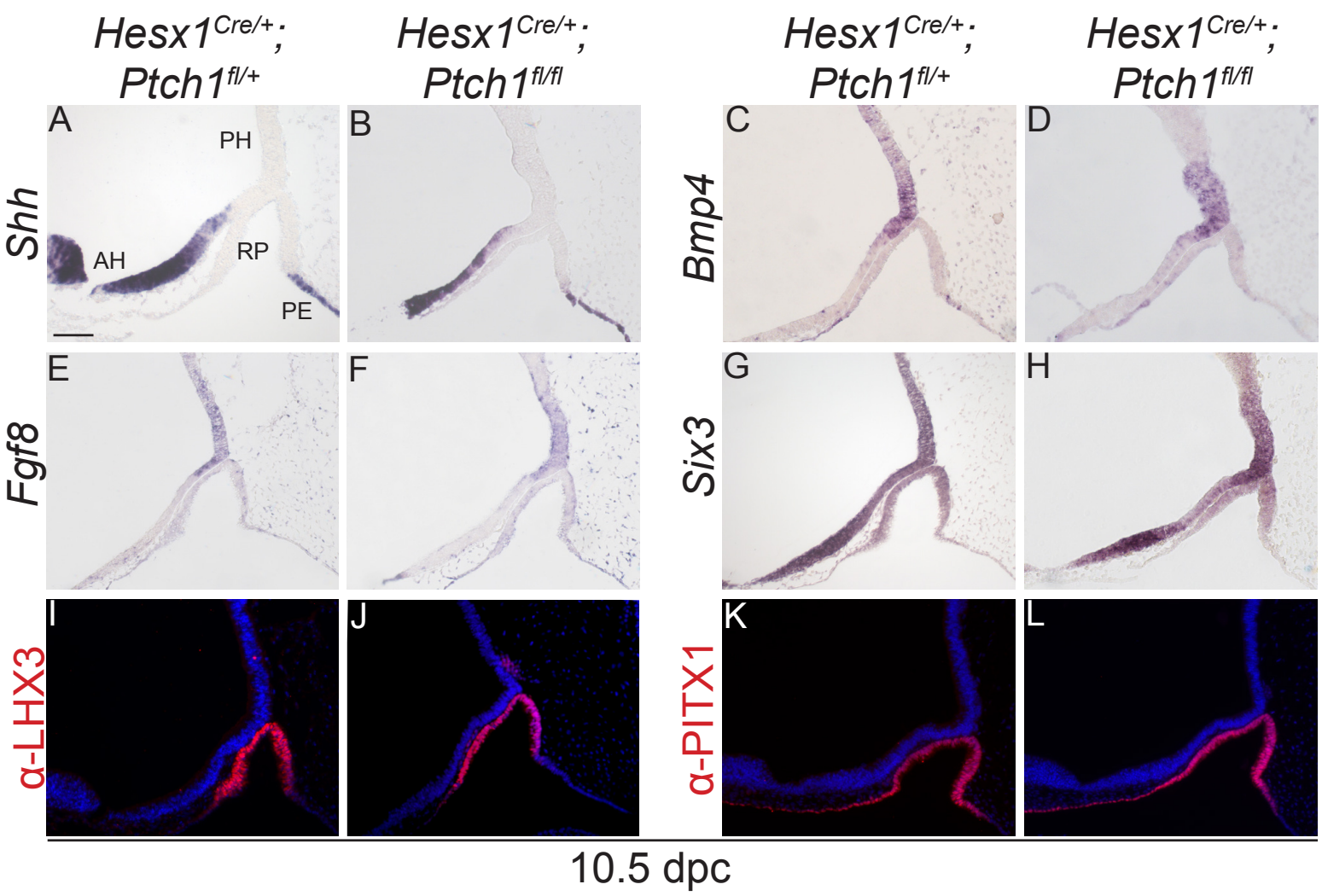

Figure S12. Patterning of the developing hypothalamus and Rathke's pouch is not affected in *Hesx1*$^{Cre/+}$;*Ptch1*$^{fl/fl}$ mutants. (A-L) *In situ* hybridisation (A-H) and immunofluorescence (I-L) on mid-sagittal sections of control and *Hesx1*$^{Cre/+}$;*Ptch1*$^{fl/fl}$ mutant embryos at 10.5 dpc. Markers are indicated. Note the comparable expression patterns of all markers analysed between genotypes. Abbreviations as in SFig. 2. Scale bar: 100μm

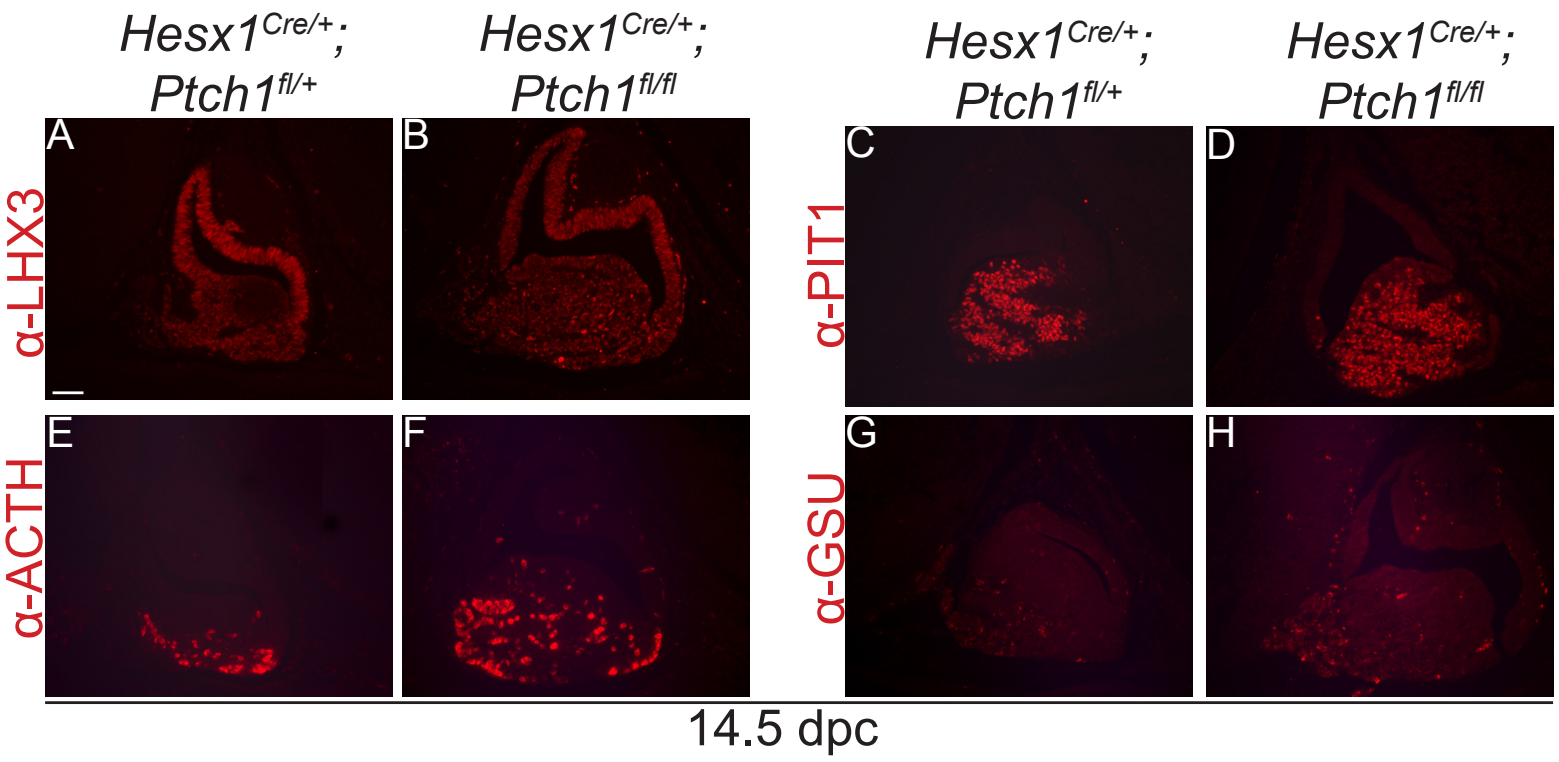

Figure S13. LHX3, ACTH, PIT1 and α-GSU are expressed in the developing pituitary of *Hesx1*$^{Cre/+}$;*Ptch1*$^{fl/fl}$ mutants. (A-H) Immunofluorescence on mid-sagittal histological sections of control and *Hesx1*$^{Cre/+}$;*Ptch1*$^{fl/fl}$ mutant embryos at 14.5 dpc. Note the enlargement of the expression domains of the markers analysed in the mutants relative to the control embryos. Scale bar: 100μm

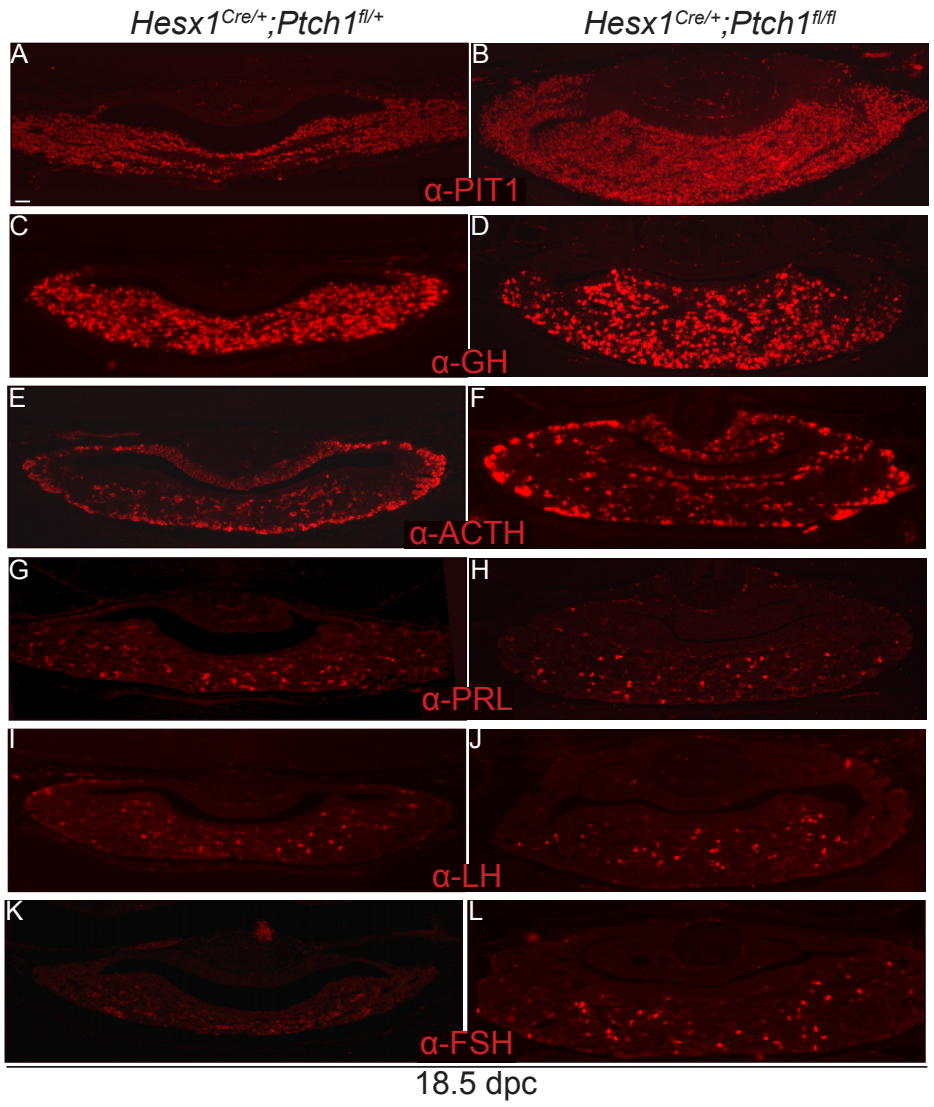

Figure S14. Hormone-producing cells are generated in the *Hesx1*$^{Cre/+}$;*Ptch1*$^{fl/fl}$ mutants at 18.5dpc. Immunofluorescence on frontal histological sections, at the level of the pituitary gland, in 18.5 dpc mutants and control embryos. Note the presence of PIT1+ve (somato, lacto and thyro -troph), GH+ve (somatotroph), ACTH+ve (cortico and melano -troph), PRL+ve (lactotrophs), LH+ve and FSH+ve (gonadotroph) cells in the mutant pituitary. Scale bars: 100μm.

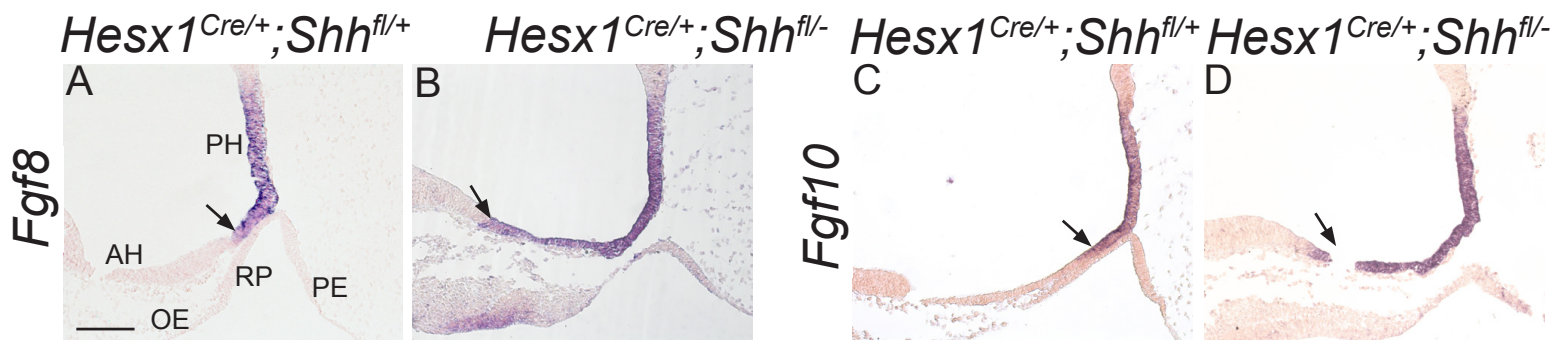

Figure S15. *Fgf8* and *Fgf10* are co-expressed in the developing hypothalamus. *In situ* hybridisation on mid-sagittal sections of *Hesx1*$^{Cre/+}$;*Shh*$^{fl/-}$ mutants and control embryos at 10.5 dpc. Note the co-expression of these two markers in the control and mutant embryos and the expansion of the *Fgf8/Fgf10* expression domains (arrows). Abbreviations as in SFig. 2.